

Scanning Tunneling Microscopy of Ordered Arrays of Heteropolyacids Deposited on a Graphite Surface

I. K. Song,^{†,§} M. S. Kaba,[†] G. Coulston,[‡] K. Kourtakis,[‡] and M. A. Barteau^{*,†}

Center for Catalytic Science and Technology, Department of Chemical Engineering, University of Delaware, Newark, Delaware 19716, and Central Research and Development Department, E. I. duPont de Nemours and Company, Wilmington, Delaware 19880

Received March 6, 1996. Revised Manuscript Received May 9, 1996[⊗]

Keggin-type heteropolyacids (water-soluble $H_3PMo_{12}O_{40}$, $H_4PMo_{11}VO_{40}$, and $H_8PMo_{10}VCuO_{40}$ and water-insoluble $K_3PMo_{12}O_{40}$ and $H_{3-x}Cs_xPMo_{12}O_{40}$, $x = 1, 2, 2.5, 3$) deposited on highly oriented pyrolytic graphite (HOPG) surfaces were successfully imaged by scanning tunneling microscopy (STM). All of these heteropoly acids (HPAs) formed clear two-dimensional ordered arrays on graphite, and their periodicities were in good agreement with values determined by X-ray crystallography. Spatially resolved tunneling spectroscopy was used to demonstrate that the arrays imaged represented HPA monolayers, as the characteristic tunneling spectrum of graphite was obtained at high-symmetry interstitial sites in these arrays. The periodicity of the ordered arrays of the water-soluble Keggin-type HPAs was ca. 10–11 Å. However, ordered arrays of the water-insoluble $K_3PMo_{12}O_{40}$ and $H_{3-x}Cs_xPMo_{12}O_{40}$ showed periodicities of ca. 12–14 Å, values somewhat larger than that of the pure acid form. The array spacing increased monotonically with increasing substitution of larger (Cs) cations, as expected. However, the nearly invariant periodicity of 2-D arrays of the water-soluble HPAs with changes in the number of protons suggests that there is little or no water of crystallization in these arrays, in contrast to the bulk compounds. STM permitted observation of the ordered structures of HPAs when deposited on a chemically inert surface, as well as the determination of the effects of changing framework and charge-compensating cations on these structures. The ubiquity of ordered array formation of these HPAs suggests that they can be utilized to create well-defined surfaces with more complex chemical functions than one typically encounters in studies of metal or oxide single-crystal surfaces.

Introduction

STM permits surfaces to be imaged at the atomic level.^{1–3} Although the emphasis of much early STM work was on the study of semiconductor surfaces,^{4–6} it has been used to image graphite, metals, and superconductors.⁷ Many insulating materials such as proteins,⁸ liquid crystals,⁹ petroleum asphaltenes,¹⁰ and Langmuir–Blodgett films¹¹ have also been imaged successfully using STM by depositing the molecules on

a conducting substrate. A previous study from this group¹² was one of the first two reports^{12,13} of the formation and the imaging of ordered arrays of heteropolyacids (HPAs) deposited on conductive surfaces such as graphite.

HPAs as both acid catalysts^{14,15} and oxidation catalysts^{16–18} have been widely investigated and have been used in a commercial process producing methacrylic acid.¹⁹ HPAs are very attractive catalysts because (1) the acidic and redox properties can be controlled in a systematic way and (2) owing to their ability to form a pseudo-liquid phase, catalytic reactions sometimes proceed not only on the surface but also in the bulk of these solids.²⁰

The size of $PMo_{12}O_{40}^{3-}$, the typical Keggin-type²¹ anion, is ca. 10–12 Å as determined by X-ray crystal-

[†] University of Delaware.

[‡] E. I. duPont de Nemours and Co.

[§] Present address: Department of Industrial Chemistry, Kangnung National University, Kangnung, Kangwondo 210-702, Korea.

* To whom correspondence should be addressed Tel: 302-831-8905, Fax: 302-831-2085, E-Mail: barteau@che.udel.edu

[⊗] Abstract published in *Advance ACS Abstracts*, July 1, 1996.

(1) Binnig, G.; Rohrer, H.; Gerber, C.; Weibel, E. *Phys. Rev. Lett.* **1982**, *49*, 57.

(2) Binnig, G.; Rohrer, H. *Surf. Sci.* **1983**, *126*, 236.

(3) Binnig, G.; Rohrer, H.; Gerber, C.; Weibel, E. *Phys. Rev. Lett.* **1983**, *50*, 120.

(4) Rohrer, G. S.; Henrich, V. E.; Bonnel, D. A. *Science* **1990**, *250*, 1239.

(5) Rohrer, G. S.; Bonnel, D. A. *J. Vac. Sci. Tech. B* **1991**, *9*, 783.

(6) Matsumoto, T.; Tanaka, H.; Kawai, T.; Kawai, S. *Surf. Sci.* **1992**, *278*, L153.

(7) Hansma, P. K.; Tersoff, J. *J. Appl. Phys.* **1987**, *61*, R1.

(8) Haggerty, L.; Watson, B. A.; Barteau, M. A.; Lenhoff, A. M. *J. Vac. Sci. Technol. B* **1991**, *9*, 1219.

(9) Mizutani, W.; Shigeno, M.; Ono, M.; Kajimura, K. *Appl. Phys. Lett.* **1990**, *56*, 1974.

(10) Watson, B. A.; Barteau, M. A. *Ind. Eng. Chem. Res.* **1994**, *33*, 2358.

(11) Loo, B. H.; Liu, Z. F.; Fujishima, A. *Surf. Sci.* **1990**, *1*, 227.

(12) Watson, B. A.; Barteau, M. A.; Haggerty, L.; Lenhoff, A. M.; Weber, R. S. *Langmuir* **1992**, *8*, 1145.

(13) Keita, B.; Chauveau, F.; Theobald, F.; Belanger, D.; Nadjo, L. *Surf. Sci.* **1992**, *264*, 271.

(14) Okuhara, T.; Nishimura, T.; Ohashi, K.; Misono, M. *Chem. Lett.* **1990**, 1201.

(15) Okuhara, T.; Kasai, A.; Hayakawa, N.; Yoneda, Y.; Misono, M. *J. Catal.* **1983**, *83*, 121.

(16) Song, I. K.; Shin, S. K.; Lee, W. Y. *J. Catal.* **1993**, *144*, 348.

(17) Komaya, T.; Misono, M. *Chem. Lett.* **1983**, 1177.

(18) Ai, M. *J. Catal.* **1984**, *85*, 324.

(19) Ai, M. *J. Catal.* **1989**, *116*, 23.

(20) Misono, M. *Catal. Rev. Sci. Eng.* **1987**, *29*, 269.

(21) Keggin, J. F. *Nature* **1933**, *131*, 908.

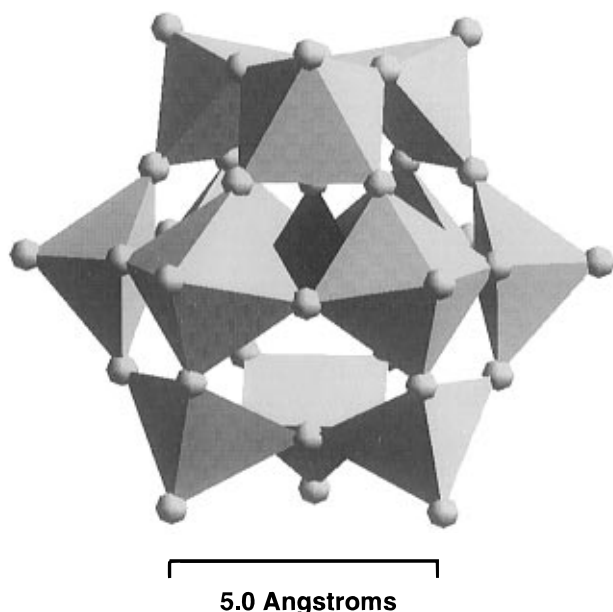


Figure 1. Polyhedral representation of the molecular structure of the Keggin anion ($\text{PMo}_{12}\text{O}_{40}$)³⁻.

lography²²⁻²⁴ and STM.¹² Figure 1 shows a polyhedral representation of the molecular structure of the Keggin-type, $\text{PMo}_{12}\text{O}_{40}$ ³⁻, heteropolyanion.²⁵ The structure of $\text{PMo}_{12}\text{O}_{40}$ ³⁻ consists of a heteroatom, P, at the center of the anion cluster, tetrahedrally coordinated to four oxygen atoms. This tetrahedron is surrounded by 12 MoO_6 octahedra.

In this work, Keggin-type HPAs and their water-insoluble salts were deposited on a graphite surface and imaged using STM, in order to examine the effects of changing framework and counteranions on the HPA structure and array characteristics observable by STM.

Experimental Section

$\text{H}_3\text{PMo}_{12}\text{O}_{40}$ was obtained from Aldrich Chem. Co. (Milwaukee, WI). The crystals were first dissolved in water and recrystallized by slow heating at 100 °C and then calcined at 300 °C for 2 h to remove water of crystallization. Cation-exchanged HPAs such as $\text{K}_3\text{PMo}_{12}\text{O}_{40}$ and $\text{H}_{3-x}\text{Cs}_x\text{PMo}_{12}\text{O}_{40}$ ($x = 1, 2, 2.5, 3$) were prepared using procedures described elsewhere.^{26,27} $\text{H}_4\text{PMo}_{11}\text{VO}_{40}$ and $\text{H}_8\text{PMo}_{10}\text{VCuO}_{40}$ were kindly supplied by the DuPont Co. (Wilmington, DE). A drop of approximately 0.01 M aqueous solution of the water-soluble HPA was deposited on a freshly cleaved HOPG surface and allowed to dry in air for ca. 45 min at room temperature. In general, we have found the formation of surface arrays of Keggin ion samples, including those reported here, to be rather insensitive to the conditions of deposition for solutions in this concentration range. Upon drying in air, one typically observes a visible polycrystalline "rind" around the original perimeter of the liquid drop; however, the enclosed region exhibits monolayer arrays of the HPA as demonstrated by STM and tunneling spectroscopy (TS) results discussed below. A few samples of other polyoxometalates (e.g., $\text{K}_{12.5}\text{Na}_{1.5}\text{[NaP}_5\text{W}_{30}\text{O}_{110}]$) exhibit a tendency to form bulk crystallites

rather than monolayer films upon drying,²⁸ and variations of the drying procedure (e.g., temperature control, use of a vacuum desiccator, etc.) may be required. However, such problems were not encountered in these studies of Keggin-type HPAs and their inorganic salts.

For the nominally water-insoluble HPA solution of $\text{K}_3\text{PMo}_{12}\text{O}_{40}$ and $\text{H}_{3-x}\text{Cs}_x\text{PMo}_{12}\text{O}_{40}$, vials containing aqueous suspensions/solutions were vigorously shaken before a drop of the very fine suspended particles was deposited on the graphite surface to dry in air. It is possible that in each ion-exchange reaction to produce a specific sample, there may have been other products of varying cation content; however, for each of these samples deposited on graphite, subsequent imaging of several different sites on the adsorbed HPA surface by STM showed ordered arrays of polyanions that had consistent periodicities, and tunneling spectroscopy measurements on these anions yielded negative differential resistance (NDR) behavior¹² at consistent values of the applied potential. HPAs are known to exhibit NDR behavior in their tunneling spectra and the potential at which this behavior is observed can be used as a fingerprint of the HPA.¹² Both the array spacing and NDR peak voltage were found to vary for samples in which the proton content was deliberately varied by ion exchange, e.g., for the series $\text{H}_{3-x}\text{Cs}_x\text{PMo}_{12}\text{O}_{40}$.²⁹ The absence of such variations among different regions of the same sample probed by STM and TS suggests that the composition of the surface HPA arrays is spatially uniform. In agreement with other STM reports,^{12,29} the TS measurements also indicated that these HPAs formed monolayers on the graphite surfaces.

STM images were obtained both in air and in a N_2 -filled glovebox using a Topometrix (Santa Clara, CA) TMX 2010 instrument. The images and tunneling spectra for these samples did not exhibit noticeable sensitivity to the ambient conditions. The results reported here were obtained over a period of months, during which the relative humidity of the laboratory ranged up to 60%. Samples imaged under these conditions were not distinguishable from those obtained in the humidity-free environment of the glovebox.

Mechanically formed Pt/Ir tips were used in all experiments. The quality and stability of the tips were first established by scanning the bare graphite section of the surface repeatedly in air or in the glovebox. The tip was considered "good" if it reproduced atomic resolution images of the graphite surface from scan to scan taken at at least three different spots on the graphite surface and if the periodicities of these atoms determined from two-dimensional fast fourier transforms (2-D FFT) were within 0.2 Å of the 2.5 Å periodicity of graphite. The "good" tip would then be positioned over an adsorbate-covered region of the surface. Images were obtained in the constant-current mode at a positive sample bias of 100 mV and a tunneling current of 1–2 nA. None of the STM images presented in this work was filtered, and all lattice dimensions reported are average values determined by performing fast fourier transform analyses on at least three different images obtained at different locations on the sample; each image was acquired using a different tip. Tunneling spectra were obtained by positioning the tip at the desired location, and then ramping the sample bias from –2 to +2V with respect to the tip while monitoring the tunneling current. Twelve-to-fifteen repetitions of the TS measurement were made with each tip to ensure reproducibility. In addition, we have reproduced these HPA tunneling spectra using a second STM instrument. As with the images, little variation in tunneling spectra was observed, whether the measurements were made in the laboratory atmosphere or in an N_2 -filled glovebox.

Results and Discussion

Using the STM, we successfully imaged arrays of different Keggin-type HPAs. Figure 2 shows an STM image of a typical Keggin-type HPA, $\text{H}_3\text{PMo}_{12}\text{O}_{40}$, along

(22) Highfield, J. G.; Moffat, J. B. *J. Catal.* **1984**, *88*, 177.

(23) Izumi, Y.; Hasebe, R.; Urabe, K. *J. Catal.* **1983**, *84*, 402.

(24) Bradley, A. J.; Illingsworth, J. W. *Proc. R. Soc. London A* **1936**, *157*, 113.

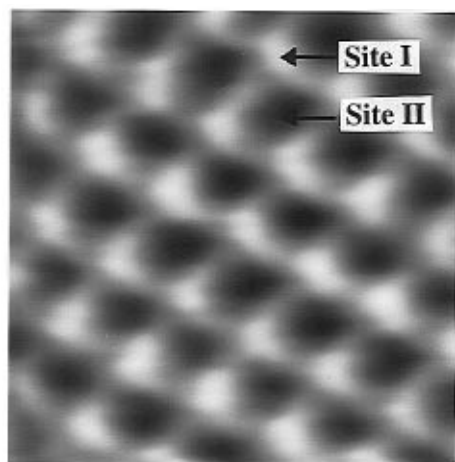
(25) Pope, M. T. *Heteropoly and Isopoly Oxometalates*; Springer-Verlag: New York, 1983.

(26) Okuhara, T.; Nishimura, T.; Watanabe, H.; Misono, M. *J. Mol. Catal.* **1992**, *74*, 247.

(27) Tatematsu, S.; Hibi, S.; Okuhara, T.; Misono, M. *Chem. Lett.* **1984**, 865.

(28) Kaba, M. S.; Song, I. K.; Duncan, D. C.; Hill, C. L.; Barteau, M. A. *J. Am. Chem. Soc.*, submitted.

(29) Kaba, M. S.; Song, I. K.; Barteau, M. A., in preparation.



5.07 nm x 5.07 nm

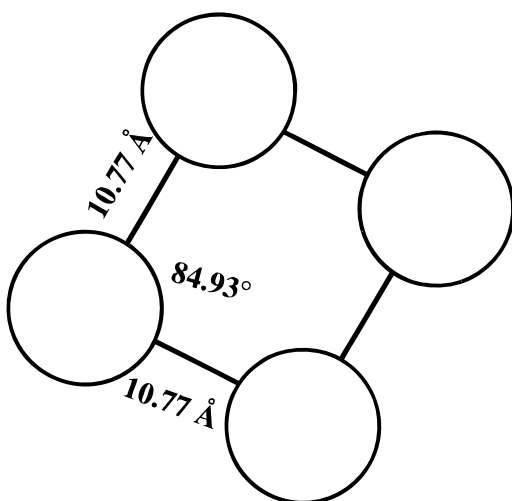
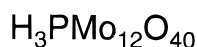


Figure 2. STM image and schematic diagram of the unit cell of $\text{H}_3\text{PMo}_{12}\text{O}_{40}$.

with a schematic diagram of its surface unit cell. All unit cells were constructed based on lattice parameters determined by performing fast fourier transforms (FFT) on various STM images for each sample. The STM image shows a well-ordered two-dimensional array of $\text{H}_3\text{PMo}_{12}\text{O}_{40}$ with a nearly square symmetry ($\alpha = 84.93^\circ$) on graphite. The periodicity of the arrays is $10.77 \pm 0.26 \text{ \AA}$ and is in good agreement with lattice dimensions determined by X-ray crystallography.^{22–24} The STM not only allowed us to observe the formation of ordered arrays of these HPAs on a chemically inert substrate as was observed earlier,^{12,13} but it also allowed us to directly determine the molecular dimensions of the HPA.

Spatially resolved tunneling spectra demonstrate that the 2-D arrays imaged in fact represent monolayer HPA coverage of these regions of the graphite surface. Figure 3 shows tunneling spectra obtained at the positions labeled “site I” and “site II” on the image of the $\text{H}_3\text{PMo}_{12}\text{O}_{40}$ array in Figure 2. With the tip positioned atop the corrugations in the Keggin ion array (site I), one reproducibly observes tunneling spectra characteristic of the heteropolyanion. The key features are the presence of a broad-bandgap region (i.e., a flat $I-V$ curve

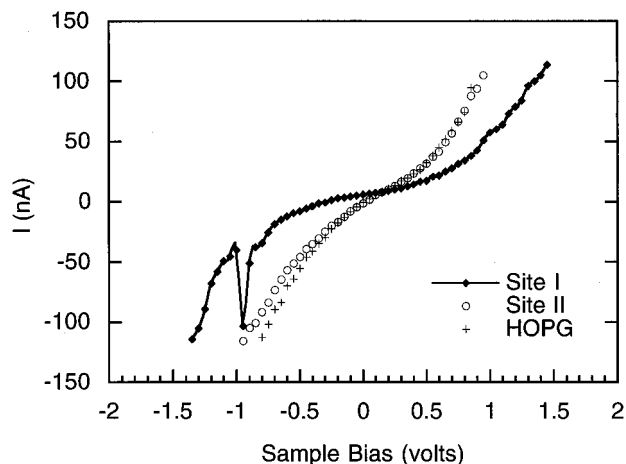


Figure 3. Tunneling spectra of the $\text{H}_3\text{PMo}_{12}\text{O}_{40}$ arrays obtained at the positions indicated in Figure 2, along with the tunneling spectrum from a bare graphite surface.

about the origin) and the presence of a sharp peak in the $I-V$ spectrum (at -0.95 V in this example) characteristic of negative differential resistance (NDR) behavior. We have previously demonstrated NDR in tunneling spectra of heteropoly and isopolyanion arrays on graphite¹² and have observed this phenomenon for more than 12 different polyoxometalates.²⁹ In fact, the applied voltage at which NDR is observed appears to vary systematically with the reduction potential of the HPA²⁹ and thus can be utilized as a site-specific probe of surface redox properties. Of equal importance for the present purposes, however, is the *absence* of such features in tunneling spectra obtained at high-symmetry “hollow” sites in the array (e.g., “site II” in Figure 2). Tunneling spectra at this position exhibit greater conductivity at all applied potentials, positive and negative, than those measured atop the anions. In fact, the tunneling spectra obtained at these interstitial positions were indistinguishable from those measured on a bare graphite surface. The fact that one can “see” the underlying graphite at the interstitial positions in the heteropolyanion array demonstrates that the array consists of a single HPA monolayer, as we have previously shown¹² for the isopolyanion compound $(\text{NH}_4)_6\text{V}_{10}\text{O}_{28} \cdot 6\text{H}_2\text{O}$.

Figure 4 shows STM images of several cation-exchanged HPAs along with schematic diagrams of the unit cells derived from these images. The images clearly show two-dimensional ordered arrays of HPAs on the graphite surface. HPAs in the solid crystalline state are composed of heteropolyanions (the primary structure), cations (protons and metals), water of crystallization, and/or organic molecules. A schematic of this three-dimensional arrangement, called the secondary structure,²⁰ is shown in Figure 5. Models^{30,31} of the secondary structure of HPAs constructed to account for NMR results suggest that the secondary structure of bulk $\text{H}_3\text{PW}_{12}\text{O}_{40} \cdot 6\text{H}_2\text{O}$ ($=(\text{H}_5\text{O}_2)_3\text{PW}_{12}\text{O}_{40}$) is one in which the polyanions are connected by $\text{H}^+(\text{H}_2\text{O})_2$ bridges. The secondary structure of $\text{Cs}_3\text{PMo}_{12}\text{O}_{40}$ is presumably similar except that each $\text{H}^+(\text{H}_2\text{O})_2$ is replaced by Cs^+ .

(30) Brown, G. M.; Noe-Spirlet, M. R.; Busing, W. R.; Levy, H. A. *Acta Crystallogr.* **1977**, *B33*, 1038.

(31) Misono, M. *Proc. New Frontiers in Catalysis, 10th Int. Cong. Catal., July 1992 (Budapest, Hungary)*; Gucci, L.; Solymosi, F.; Tetenyi, P., Eds.; Elsevier Science: Amsterdam, 1992; p 69.

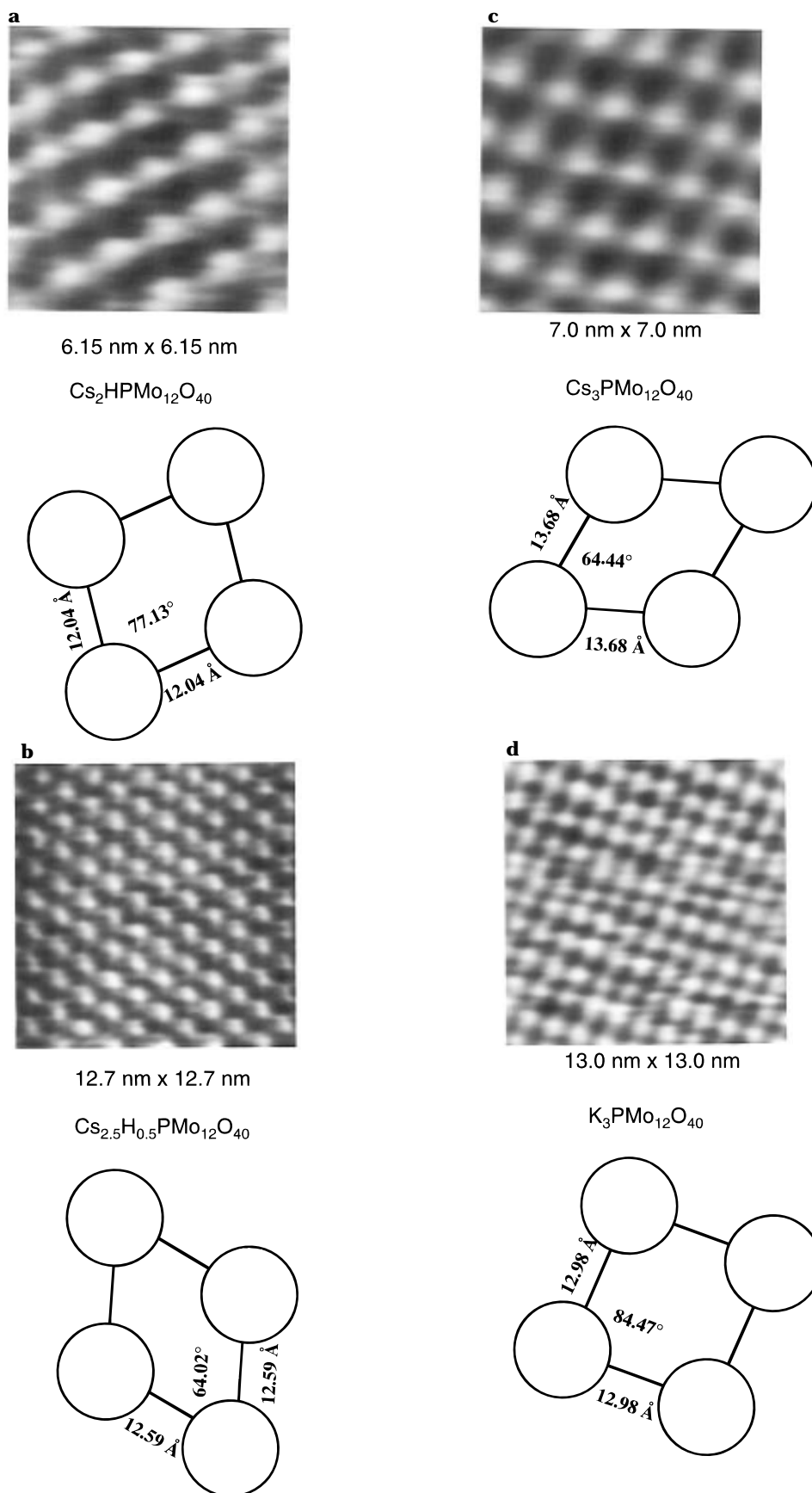


Figure 4. STM images and schematic diagrams of the unit cells of arrays of (a) $\text{Cs}_2\text{HPMo}_{12}\text{O}_{40}$, (b) $\text{Cs}_{2.5}\text{H}_{0.5}\text{PMo}_{12}\text{O}_{40}$, (c) $\text{Cs}_3\text{PMo}_{12}\text{O}_{40}$, and (d) $\text{K}_3\text{PMo}_{12}\text{O}_{40}$.

As bulk solids, the pure acid forms of the HPAs and their water-soluble salts contain large amounts of water at room temperature and their crystal forms strongly

depend on this water of crystallization. The bulk structures of $[\text{PMo}_{12}\text{O}_{40}]^{3-}$ derivatives are not as well defined as those of their $[\text{PW}_{12}\text{O}_{40}]^{3-}$ counterparts, and

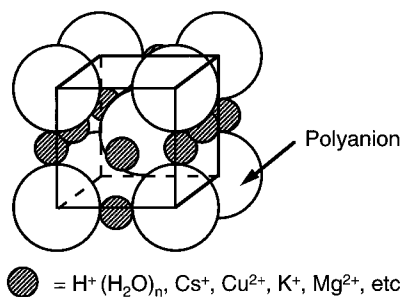


Figure 5. Secondary structure of heteropoly acids, after Misono.²⁰

even here there is some variation in literature reports. The basic trends in lattice dimensions with thermal dehydration of hydrated heteropolyacids are not in dispute, however. Brown et al.³⁰ reported the most comprehensive structural study by XRD of $\text{H}_3\text{PW}_{12}\text{O}_{40} \cdot 6\text{H}_2\text{O}$. The nearest center-to-center distance between the $[\text{PW}_{12}\text{O}_{40}]^{3-}$ anions was 10.831 Å.³⁰ Izumi et al.³² list three crystal forms of 12-tungstophosphoric acid: $\text{H}_3\text{PW}_{12}\text{O}_{40} \cdot 5\text{H}_2\text{O}$, $\text{H}_3\text{PW}_{12}\text{O}_{40} \cdot 14\text{H}_2\text{O}$, and $\text{H}_3\text{PW}_{12}\text{O}_{40} \cdot 29\text{H}_2\text{O}$. Of these, $\text{H}_3\text{PW}_{12}\text{O}_{40} \cdot 29\text{H}_2\text{O}$ is claimed to be the most stable form at room temperature and its lattice is face-centered cubic with a primitive cell volume of ca. 1590 Å³ (and an anion center-to-center distance of 13.10 Å).³² On the other hand, the crystal form of $\text{H}_3\text{PW}_{12}\text{O}_{40} \cdot 5\text{H}_2\text{O}$ (which is most likely actually the hexahydrate³⁰) is reported to be body-centered cubic with a primitive cell volume of 900 Å³ and an anion center-to-center distance of 10.53 Å.³² Another X-ray structure analysis²⁴ showed that the 29 water molecules in $\text{H}_3\text{PW}_{12}\text{O}_{40} \cdot 29\text{H}_2\text{O}$ form a cluster with the three protons ($\text{H}_3(\text{H}_2\text{O})_{29}^{3+}$) and these clusters and the polyanion clusters appear at alternate corners of the body-centered cubic lattice, and the heteropolyanion and hydrated proton clusters are each 10.10 Å in diameter, assuming that each of the clusters is spherical. The water of crystallization can be removed stepwise with increasingly severe thermal treatment,³³ and a somewhat more stable crystalline form can exist at each step of the dehydration process. Most of the water molecules in the water-soluble HPAs are removed at 100–150 °C.^{33,34} In the case of water-insoluble salts of HPAs such as K^+ - and Cs^+ -exchanged HPAs, the number of water molecules is much smaller and water can be removed by drying in vacuum at 25 °C.³³

In bulk form, water-soluble HPAs and their water-soluble salts typically have surface areas of less than 10 m²/g, while water-insoluble HPA salts such as $\text{K}_3\text{PMo}_{12}\text{O}_{40}$ and $\text{Cs}_3\text{PMo}_{12}\text{O}_{40}$ have surface areas greater than 40 m²/g.³⁵ The large surface areas of the water-insoluble HPAs may be due to their unique secondary structures. It has been reported³⁵ that the water-insoluble HPAs behave like porous catalysts such as zeolites because of their stable three-dimensional secondary structure.

Unlike the bulk crystals, the two-dimensional ordered HPA arrays on graphite appear to be unaffected by water of crystallization or by their solubility properties

Table 1. Periodicities of Cation-Exchanged Heteropolyacids

heteropolyacid/salt	periodicity of array, Å
$\text{H}_3\text{PMo}_{12}\text{O}_{40}$	10.77 ± 0.26
$\text{HCs}_2\text{PMo}_{12}\text{O}_{40}$	12.04 ± 0.22
$\text{H}_{0.5}\text{Cs}_{2.5}\text{PMo}_{12}\text{O}_{40}$	12.59 ± 0.05
$\text{K}_3\text{PMo}_{12}\text{O}_{40}$	12.98 ± 0.16
$\text{Cs}_3\text{PMo}_{12}\text{O}_{40}$	13.68 ± 0.14

in water. Table 1 lists the periodicities of the arrays of HPAs shown in the STM images of Figures 2 and 4. Comparison of these periodicities indicates that the periodicity of the ordered arrays of $\text{H}_{3-x}\text{Cs}_x\text{PMo}_{12}\text{O}_{40}$ increases with increasing Cs content. Comparison of the periodicities of the arrays of the water-insoluble HPAs ($\text{K}_3\text{PMo}_{12}\text{O}_{40}$ and $\text{Cs}_3\text{PMo}_{12}\text{O}_{40}$) and of the water-soluble HPA, $\text{H}_3\text{PMo}_{12}\text{O}_{40}$, likewise shows that the periodicities of the arrays of the water-insoluble HPAs are larger. This result indicates that even though the bulk crystals of the water-soluble HPA contain more water of hydration than its water-insoluble counterparts, this is not, however, reflected in the STM images. Perhaps the water molecules are more stable within the three-dimensional structure of the bulk crystals than in the two-dimensional structure of HPA arrays on the graphite surface. The number of water molecules in the two-dimensional arrays may be very small and may not appreciably affect the periodicities of the ordered arrays of HPAs. Also, models of the secondary structure of HPAs³¹ suggest that the insoluble cations such as K^+ and Cs^+ exist in the interstices between the polyanions, acting as bridges, just as the protons do in the pure acid form. We conclude, therefore, that the increase of 1–2 Å in the periodicities of the arrays of the water-insoluble HPAs in the STM images is due to the introduction of large cations such as K^+ (ionic radius of 1.33 Å) and Cs^+ (ionic radius of 1.67 Å) in place of the bridging protons in the pure acid form.

Aqueous HPA solutions were deposited on the graphite surfaces and allowed to dry at room temperature in this work; the deposited samples did not undergo any other physical treatment nor any chemical treatment to remove water. Also, the STM images were obtained both in air and in a glovebox. These procedures might lead one to expect that the HPAs deposited from aqueous solution would retain large amounts of water in the interstices after drying; however, as noted, this appears not to be the case for the 2-D surface arrays. Hence, the increase in periodicities of the arrays of the water-insoluble HPAs on HOPG can be attributed only to the effect of the cations in these HPAs, suggesting that one can control the size of the interstitial space between the polyanions by a judicious choice of the counter ion. Such STM images provide important insights into the characteristics of supported heteropolyacids on the molecular level with potential applications as acid and oxidation catalysts.

Figure 6 shows STM images of heteropolyacids with different frameworks (changing molybdenum content), $\text{H}_4\text{PMo}_{11}\text{VO}_{40}$ and $\text{H}_8\text{PMo}_{10}\text{VCuO}_{40}$. These HPAs also form well-ordered two-dimensional arrays on the graphite surface, which may be compared with the ordered $\text{H}_3\text{PMo}_{12}\text{O}_{40}$ arrays on HOPG in Figure 2. In bulk crystals of HPAs, the number of molecules of water of crystallization has a very strong effect on the three-dimensional secondary structure of the HPA.^{30–32} For

(32) Izumi, Y.; Urabe, K.; Onaka, M. *Zeolite, Clay, and Heteropoly Acid in Organic Reactions*; Kodansha: Tokyo, 1992.

(33) Otake, M.; Onodo, T. *Shokubai* **1975**, 17, 13.

(34) Misono, M.; Konishi, Y.; Furuta, M.; Yoneda, Y. *Chem. Lett.* **1978**, 709.

(35) Okuhara, T.; Nishimura, T.; Misono, M. *Chem. Lett.* **1995**, 155.

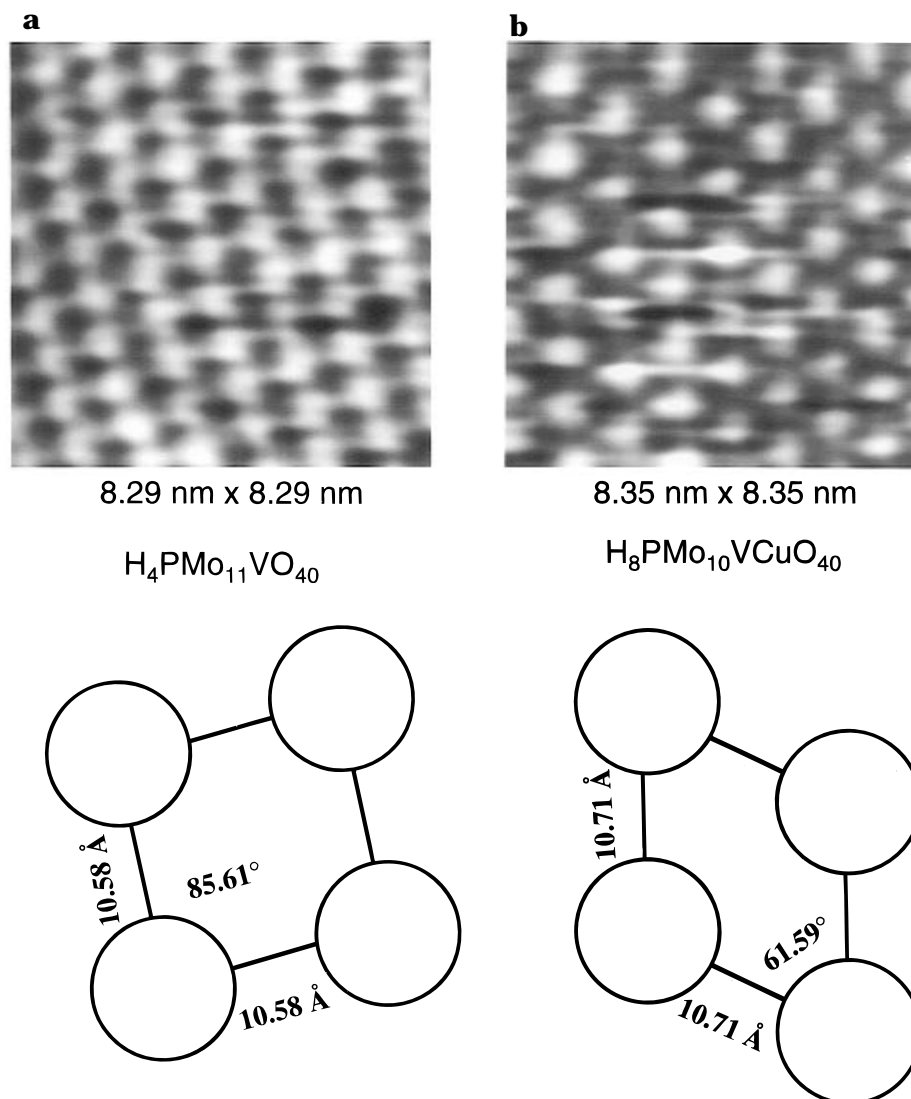


Figure 6. STM images and schematic diagrams of the unit cells of arrays of (a) $\text{H}_4\text{PMo}_{11}\text{VO}_{40}$ and (b) $\text{H}_8\text{PMo}_{10}\text{VCuO}_{40}$.

Table 2. Periodicities of Heteropolyacids with Different Framework Compositions

heteropolyacid	periodicity of array, Å
$\text{H}_3\text{PMo}_{12}\text{O}_{40}$	10.77 ± 0.26
$\text{H}_4\text{PMo}_{11}\text{VO}_{40}$	10.58 ± 0.44
$\text{H}_8\text{PMo}_{10}\text{VCuO}_{40}$	10.71 ± 0.36

example, the eight protons in $\text{H}_8\text{PMo}_{10}\text{VCuO}_{40}$ would be expected to bind more water molecules than the four protons in $\text{H}_4\text{PMo}_{11}\text{VO}_{40}$. Even though changing the framework of the HPA resulted in changes in the number of charge-compensating protons (and thus the potential number of hydrated protons), the periodicities of the arrays of these HPAs with different frameworks, shown in Table 2, are almost identical. Therefore, changing the framework composition of the heteropolyacid results in no significant change in the periodicities of the ordered arrays formed by the HPAs in the STM images. This observation is consistent with the results³⁶ of XRD measurements of anion structure for single crystals of $\text{H}_{2.6+x}\text{Cu}_{0.2}(\text{PV}_x\text{Mo}_{12-x}\text{O}_{40})$, $x = 1, 2,$ and 3 . These results also support the conclusion that, unlike

its effect on the three-dimensional structure of bulk crystals, water of crystallization has an insignificant impact on the periodicities of arrays of HPAs on the graphite surface. Indeed it is reasonable to conclude that little or no water of crystallization is present in these two-dimensional surface arrays.

Conclusions

Water-soluble Keggin-type HPAs and their water-insoluble salts deposited on a graphite surface were successfully imaged by STM. It was found that all the HPAs formed two-dimensional ordered arrays on the substrate. Spatially resolved tunneling spectroscopy demonstrated that these arrays were HPA monolayers. The periodicities of the arrays of $\text{H}_3\text{PMo}_{12}\text{O}_{40}$, $\text{H}_4\text{PMo}_{11}\text{VO}_{40}$, and $\text{H}_8\text{PMo}_{10}\text{VCuO}_{40}$ were ca. 11 Å. These results indicate that changing framework composition in the HPA structure produces almost no change in the periodicities of the ordered arrays formed on graphite, even when the net charge (and the number of charge-compensating protons) is changed. However, water-insoluble K^+ - and Cs^+ -exchanged HPAs showed periodicities of 12–14 Å, indicating that the introduction

(36) Herzog, B.; Bensch, W.; Ilkenhans, Th.; Schlogl, R. *Catal. Lett.* **1993**, *20*, 203.

of large cations such as K^+ and Cs^+ in the interstices between the polyanions leads to increases in the periodicities of the ordered arrays. All of the periodicities measured by STM were calibrated against the periodicity of graphite and are in good agreement with molecular dimensions determined by X-ray crystallography. Finally, unlike bulk crystals, there is no evidence for water of crystallization affecting the periodicity of the arrays of HPA molecules on the HOPG surface.

Acknowledgment. The authors acknowledge the Korea Science and Engineering Foundation (KOSEF) for its support and the DuPont Co. for the donation of some of the heteropolyacids used. Funding for this research was provided by the National Science Foundation (Grant CTS 9410965). The Topometrix 2010 STM was acquired via an equipment grant from the U.S. Department of Energy.

CM960177L